

**Repair of Damaged Concrete Structures Using Prepreg Composites**

**(MBTC 2033)**

Guoqiang Li, Ph.D.  
Assistant Professor-Research  
Department of Mechanical Engineering  
Louisiana State University  
Baton Rouge, LA 70803

Su-Seng Pang, Ph.D., P.E.  
Jack Holmes Professor  
Department of Mechanical Engineering  
Louisiana State University  
Baton Rouge, LA 70803

The contents of this report reflect the views of the author, who is responsible for the facts and accuracy of the information presented herein. This document is disseminated under the sponsorship of the Department of Transportation, University Transportation Centers Program, in the interest of information exchange. The U.S. Government assumes no liability for the contents or use thereof.

<b>REPORT DOCUMENTATION PAGE</b>			Form Approved OMB No. 0704-0188	
Public reporting burden for this collection of information is estimated to average 1 hour per response, including the time for reviewing instructions, searching existing data sources, gathering and maintaining the data needed, and completing and reviewing the collection of information. Send comments regarding this burden estimate or any other aspect of this collection of information, including suggestions for reducing this burden, to Washington Headquarters Services, Directorate for Information Operations and Reports, 1215 Jefferson Davis Highway, Suite 1204, Arlington, VA 22202-4302, and to the Office of Management and Budget, Paperwork Reduction Project (0704-0188), Washington, DC 20503.				
1. AGENCY USE ONLY (Leave Blank)		2. REPORT DATE 07/08/2003		3. REPORT TYPE AND DATES COVERED Final report (07/01/02 – 06/30/03)
4. TITLE AND SUBTITLE Repair of Damaged Concrete Structures Using Prepreg Composites			5. FUNDING NUMBERS MBTC 2033	
6. AUTHOR(S) Guoqiang Li and Su-Seng Pang				
7. PERFORMING ORGANIZATION NAME(S) AND ADDRESS(ES) Mack-Blackwell Transportation Center 4190 Bell Engineering Center University of Arkansas Fayetteville, AR 72701			8. PERFORMING ORGANIZATION REPORT NUMBER	
9. SPONSORING/MONITORING AGENCY NAME(S) AND ADDRESS(ES) US Department of Transportation Research and Special Programs Administration 400 7 <sup>th</sup> Street, S.W. Washington, DC 20590-0001			10. SPONSORING/MONITORING AGENCY REPORT NUMBER	
11. SUPPLEMENTARY NOTES  Supported by a grant from the U.S. Department of Transportation University Transportation Centers program				
12a. DISTRIBUTION/AVAILABILITY STATEMENT			12b. DISTRIBUTION CODE  N/A	
13. ABSTRACT (MAXIMUM 200 WORDS) <p>In this study, two fast curing resins were used to repair predamaged RC columns. They were 1.5-hour heat activated curing prepreg and 20-minute ultraviolet curing resin. A 24-hour curing epoxy was also used for comparison purposes. A total of 24 steel reinforced <math>\phi</math> 152.4 mm <math>\times</math> 609.6 mm small-scale concrete columns were designed, cast, cured, surface prepared, and predamaged. The damaged samples were repaired using the three types of E-glass fabric reinforced resins. An accelerated conditioning using boiling seawater and ultraviolet radiation was also conducted to investigate the hydrothermal durability of the repaired samples. Uniaxial compression test was conducted on both control samples and conditioned samples. The test results and cost/benefit analysis results show that the two fast curing resins can replace the currently used long-time curing resins in repairing damaged RC columns.</p> <p>A finite element analysis using ANSYS was also conducted to investigate the effect of fiber orientation on the stress-strain distributions of FRP wrapped concrete columns. A total of twenty-one <math>\phi</math> 152.4 mm <math>\times</math> 304.8 mm concrete columns were prepared and tested to validate the analysis. The test and analysis results show that aligning some fibers in axial direction may be more preferable for real columns.</p>				
14. SUBJECT TERMS			15. NUMBER OF PAGES 34	
			16. PRICE CODE N/A	
17. SECURITY CLASSIFICATION OF REPORT  none	18. SECURITY CLASSIFICATION OF THIS PAGE  none	19. SECURITY CLASSIFICATION OF ABSTRACT  none	20. LIMITATION OF ABSTRACT  N/A	

1. Report Number	2. Government Access No.	3. Recipient's Catalog No.	
4. Title and Subtitle Repair of Damaged Concrete Structures Using Prepreg Composites		5. Report Date 07/08/2003	6. Performance Organization Code
7. Author(s) Guoqiang Li and Su-Seng Pang		8. Performing Organization Report No.	
9. Performing Organization Name and Address  Mack-Blackwell Transportation Center 4190 Bell Engineering Center University of Arkansas Fayetteville, AR 72701		10. Work Unit No. (TRAVIS)	11. Contract or Grant No. MBTC 2033
12. Sponsoring Agency Name and Address US Department of Transportation Research and Special Programs Administration 400 7 <sup>th</sup> Street, S.W. Washington, DC 20590-0001		13. Type of Report and Period Covered  Final report (07/01/02-06/30/03)	
15. Supplementary Notes  Supported by a grant from the U.S. Department of Transportation University Transportation Centers program		14. Sponsoring Agency Code	
16. Abstract  In this study, two fast curing resins were used to repair predamaged RC columns. They were 1.5-hour heat activated curing prepreg and 20-minute ultraviolet curing resin. A 24-hour curing epoxy was also used for comparison purposes. A total of 24 steel reinforced $\phi$ 152.4 mm $\times$ 609.6 mm small-scale concrete columns were designed, cast, cured, surface prepared, and predamaged. The damaged samples were repaired using the three types of E-glass fabric reinforced resins. An accelerated conditioning using boiling seawater and ultraviolet radiation was also conducted to investigate the hygrothermal durability of the repaired samples. Uniaxial compression test was conducted on both control samples and conditioned samples. The test results and cost/benefit analysis results show that the two fast curing resins can replace the currently used long-time curing resins in repairing damaged RC columns.  A finite element analysis using ANSYS was also conducted to investigate the effect of fiber orientation on the stress-strain distributions of FRP wrapped concrete columns. A total of twenty-one $\phi$ 152.4 mm $\times$ 304.8 mm concrete columns were prepared and tested to validate the analysis. The test and analysis results show that aligning some fibers in axial direction may be more preferable for real columns.			
17. Key Words Prepreg, E-glass fabric, Fast repair, Wet lay-up, UV curing resin, RC column.		18. Distribution Statement  No restrictions. This document is available from the National Technical Information Service, Springfield, VA 22161	
19. Security Classif. (of this report) unclassified	20. Security Cassif. (of this page) unclassified	21. No. of Pages 34	22. Price N/A

## 1 INTRODUCTION

For the past two decades, there have been mounting concerns over the safety of the deteriorated bridges in the U.S. Among the 600,000 highway bridges in the U.S., about one-half are concrete bridges, which deteriorate due to internal reinforcement corrosion, freeze-thaw action, excessive loading, lack of maintenance, poor initial design, etc. The Federal Highway Administration (FHWA) has estimated that about 40% of these bridges are functionally or structurally deficient, and the cost estimates for maintenance to just keep the status quo are as high as \$300 billion [1]. In order to maintain an efficient highway network, these deteriorated bridges have to be strengthened/upgraded so that they can meet the same safety requirements as the bridges built today.

The 21<sup>st</sup> century mandates the use of innovative materials to retrofit and upgrade the deteriorated bridges. The external bonding of fiber reinforced plastics (FRP) sheets onto the surface of concrete columns or beams has aroused worldwide interest in strengthening and retrofitting deteriorated bridges due to the high strength/stiffness to weight ratio and excellent corrosion resistance of FRPs. Although the use of FRPs in the civil infrastructures arena has only just blossomed in the past ten years, extensive studies have been conducted. Laboratory studies and theoretical modeling are being conducted, ranging from design methods, construction techniques, mechanical properties characterization, to durability [2-13].

Currently, the wet lay-up technique using ambient environment curing resins are being used to repair damaged concrete structures. A major problem associated with this material system is its delayed opening to traffic, usually as late as seven days [8,13]. The traffic delay may result in a significant cost for road users. In addition, in the event of earthquake and other natural disasters, a seven-day wait is not acceptable to prevent further damage. For these reasons and others, it is crucial to develop fast curing resins.

A major breakthrough in repairing composite structures occurred with the development of “prepreg tape,” which is a tape consisting of fibers precoated with the polymer resin. This innovation means that the fabricator no longer has to worry about mixing the resin components in the right proportions and combining the resin with the fibers in the correct fashion. It is a semi-hardened product and comes in a variety of forms: roll, sheets, or cut forms. It can be stored for a period of 30 days at room temperature or for a period of 1 year if it is kept frozen. When used, it can be cut to any shape and is flexible enough to be wrapped to the substrate surface. If heat is applied, it can be cured from 40 minutes to 3 hours depending on the materials used and the curing process. Because of its many advantages over ambient environment curing resins, it has been widely used to repair damaged composite structures [14,15]. In light of the success of using heat activated curing prepreg to repair damaged composite structures, we propose to use it to fast repair damaged concrete structures.

Another breakthrough in composite repair comes from a new ultraviolet (UV) curing resin. Since 1980's, UV curing Aerobic Acrylic adhesive has been developed to structurally bond plastics in seconds [16,17]. Recent photocatalyst inventions have led to the development of formulations that cure with UV light, visible light, or both. Advances in photocatalysts now allow the bonding of even UV blocked clear plastics. Experiments show that repairs by light curing resins have nearly the same strength as repairs by prepreg and ambient environment

curing epoxy [18]. This represents a significant advance for industries in which product reliability, safety, and fast repair are required. Again, in light of its successful use in repairing composite structures, we propose to use it to fast repair damaged concrete structures.

In this study, we focus on the repair and rehabilitation of concrete columns. Because of corrosion of the reinforcing steel and cracking and spalling of concrete, deterioration of steel reinforced concrete (RC) columns has been a topic of concerns for years in the infrastructure community. A key step in wrapping RC columns is to determine the fiber orientation. For repairing RC beams, it is clear that fibers should be aligned along the axial direction and unidirectional FRP is generally used. For RC columns, the situation is not so obvious. The fiber orientation depends on a stress-strain distribution analysis. A number of studies have been conducted to investigate the confinement or jacketing effect of FRP wraps on the stress-strain behavior of repaired RC columns. State-of-the-art reviews on the experimental investigations can be found in the two recent review papers [19,20]. Toutanji [10] proposed an analytical model to predict the stress-strain relations of the repaired RC columns. He found that the stress-strain curve can be divided into two distinct parts. In the first region, the behavior is similar to that of plain concrete, since the lateral expansion of the confined concrete is insignificant. In the second region, the FRP is fully activated and the curve is mainly dependent on the FRP wraps. Experiments were conducted to validate the analytical model [8]. Shahawy et al. [12] used an analytical model developed by Samaan et al. [21] to predict the stress-strain curve of confined columns. They found a reasonable agreement between the test results and predicted results. They also conducted a non-linear finite element analysis. They found that the FRP layers are subjected to biaxial stress conditions, as contrary to the assumption that the FRP wraps are only subjected to a hoop tension.

Although these studies are very valuable to the structural design of FRP repaired RC columns, further studies are desired. Firstly, the stress condition in the FRP jacket is biaxial, as indicated by Shahawy et al. [12]. However, almost all the previous studies used fibers in the hoop direction [20]. The biaxial stress condition implies that it is not an optimal design to lay the fibers in hoop direction only. Obviously, further studies are required to find the optimal fiber directions. Secondly, almost all the previous studies found that the stress-strain curve of repaired columns show a distinct turning point, which corresponds to the concrete failure. After that, the FRP wraps are activated. However, it is well known that the failure of concrete under compressive load occurs gradually, particularly with the confinement of the reinforcing steels. A transition zone, instead of a sharp turning point, is needed to fully activate the FRP wraps. In another word, the stress-strain curve should contain three regions instead of two regions. Obviously, detailed studies are needed to understand the characteristics of the transition zone. Thirdly, the interfacial bonding between the FRP wraps and the concrete deserves further investigations. It is well known that, for FRP repaired RC beams, interfacial bonding plays a key role. Obviously, an in-depth understanding of the effect of the interfacial bonding on the strength and stiffness of the repaired RC columns are essential in the design and construction of the FRP wraps.

The purpose of this study is to (1) experimentally investigate the effectiveness of using heat activated curing prepreg and UV curing resin to fast repair damaged concrete columns and

(2) analytically and experimentally investigate the effect of fiber orientation on the stress-strain distributions of the repaired columns.

## 2 TEST PROCEDURE

### 2.1 Raw Materials

Three types of resins were used. One was a two-part high strength epoxy adhesive. When the two parts are mixed in a 1:1 ratio by weight, the resulting adhesive can be cured in 24 hours at a room temperature. It was used as a comparison basis in this study. The second one was an E-glass 7781 style fabric reinforced phenolic prepreg. It can be cured in 1.5 hours at 135 °C. The third one was a UV curing vinyl ester resin. It can be cured by UV light or sun light in 20 minutes. For comparison purposes, the fibers used to reinforce the epoxy and the UV curing resin were the same type of E-glass fabric used in the prepreg. The physical/mechanical properties of the raw materials used are shown in Table 1.

Table 1 Physical/Mechanical Properties of the Raw Materials Used

Materials	Viscosity at 25 °C (cps)	Tensile Strength (MPa)	Modulus of Elasticity (GPa)
Epoxy	300,000	83	3.8
UV curing resin	500	70	4.2
Prepreg	—	330	24.8
E-glass fabric	—	3,000	70.0

The concrete mix utilized Type I Portland cement, fine aggregates, sand, water, and an air-entraining admixture. Due to logistic constraints, two different mixture designs were used in this study with design strengths of 27 MPa and 36 MPa. They were designated as A and B, respectively. The corresponding mixture ratios by weight were cement : water : fine aggregate : sand : admixture = 1 : 0.48 : 3.31 : 1.97 : 0.001 and cement : water : fine aggregate : sand : admixture = 1 : 0.44 : 1.76 : 3.21 : 0.001, respectively. The test results of slump, air-content, and 28-day compressive strength are shown in Table 2. It is noted that the purpose of this study was to evaluate the effectiveness of the three FRP composites. As shown in a following section, section 2.5 Specimens Conditioning, samples using concrete A were tested without conditioning and samples using concrete B were tested with conditioning. For each case (with or without conditioning), the samples used the same batch of concrete, but with three different types of FRPs. Therefore, the effect of concrete strength on the conclusions regarding the effectiveness of the three FRPs can be neglected. The steel reinforcement had a yield strength of 414 MPa (grade 60) and elastic modulus of 200 GPa.

Table 2 Test results of concrete

Batch No.	A	B
28-day compressive strength (MPa)	26.1	35.8
Slump (cm)	15.2	5.7
Air content (%)	8.1	5.3

## 2.2 Specimen Fabrication

Two types of columns were used. The first type was steel reinforced concrete column. The second type was plain concrete column. The purpose of the first type was to investigate the effectiveness of the three FRPs. The purpose of the second type was to investigate the effect of fiber orientation on the stress-strain distributions. For the first type of samples, twenty-four reinforced concrete (RC) columns were designed, cast, and cured for 28 days in a controlled environment. The RC column dimensions were  $\phi$  152.4 mm  $\times$  609.6 mm. The longitudinal reinforcement consisted of six #4 (12.7 mm diameter) rebar. The confinement reinforcement was achieved using #3 (9.5 mm diameter) rebar, formed into circular rings spaced at 50.8 mm. The schematic cross sectional view is shown in Fig. 1 (a) and the actual longitudinal and confinement reinforcements are shown in Fig. 1 (b). This arrangement and spacing were selected to satisfy all strength, minimum steel, and maximum spacing requirements as put forth in the ACI 318 code. Two different batches of concrete were used to cast the columns. Columns C1 to C12 were cast from concrete batch A, which had a compressive strength of 27 MPa. Columns C13 to C24 were cast from batch B, which had a compressive strength of 36 MPa.

For the second type of samples, twenty-one  $\phi$  152.4 mm  $\times$  304.8 mm columns were also prepared using concrete Batch B. For this type of samples, the columns were prepared without steel reinforcement. In order to investigate the fiber orientation effect, the fabric used was unidirectional E-glass fabric. Changing the fiber angle with respect to the axial direction of the column, various fiber orientations were formed. Only UV curing FRP was used to wrap the samples.

## 2.3 Precracking of RC Columns

To simulate heavily damaged RC columns and fully display the confinement capability of FRPs, all the columns of the first type, except C1, C2, and C13, which were used to determine the ultimate capacity of the undamaged columns, were precracked by a split tensile test. The cracks were introduced by continuously loading the samples until a split tensile failure. The test was conducted by referencing ASTM C 496 standard. Figure 2 (a) shows a sample under the split tensile test and Figure 2 (b) shows the sample was cracked. It is noted that, for field columns, the damages were caused by compression and bending loads. Therefore, damages using compression or bending test would be more realistic. However, the damages by compression and bending test were difficult to control. In order to better control the damages in the samples, split tensile test was used in this study. It is worth mentioning, however, the purpose of this study was to compare the effectiveness of the three FRPs. Because each sample was subjected to the same type and nearly the same amount of damage, the effect of the load type on the conclusions can be neglected.

For the second type of samples, no predamage was used.

## 2.4 Repair of Samples

For the first type of samples, the dust and floating aggregates were removed using an angle grinder after precracking, and the samples were ready to be repaired. Two repair procedures were used in this study. For the epoxy resin and the UV curing resin, the wet lay-up technique was used. This technique started with applying a layer of resin (about 300 g/m<sup>2</sup> for epoxy and about 200 g/m<sup>2</sup> for UV curing resin) to the surface of the concrete column. Next, an

E-glass fabric of 558 mm long (in axial direction) by 530 mm wide (in hoop direction) was wrapped to fully cover the resin. 50 mm extra length was used in the hoop direction to provide an overlap. A roller was then used to remove the entrapped air bubbles and press the resin to penetrate into the fabric. The roller was continuously used until the resin was reflected on the surface of the fabric, a sign of fully wetting. On the top of the fabric, another layer of resin was applied. This completed one FRP repair layer. The procedure was repeated to apply the subsequent layers. A total of two FRP layers were used in this study. It is noted that when using the UV curing resin, no roller was used. The viscosity of the resin was proper to wet through the fabric without excessive running. After wrapping, the epoxy repaired samples remained in the lab for curing. The samples were cured for 24 hours. The UV curing resin repaired samples were brought outdoors and exposed to direct sunlight. Because only one-third of the surface was exposed to the sunshine, the samples were turned every five minutes to get a uniform curing. The total time required for curing was thus extended from 20 minutes to 1 hour. It is worth mentioning that the curing by sunlight was not the only choice. The UV curing resin, as indicated by its name, is designed to be cured by UV light. Actually, for field application where direct sunlight is not available (night, shadow, etc.), UV lamps are the preferred choice. An advantage of UV lamps over sunlight is that it can be used at any time of the day, regardless of the weather. In this study, direct sunlight was available and thus was used to cure the resin. For the repair using heat activated curing prepreg, the procedure developed in joining composite beams was used [14,22]. In this technique, a piece of 558 mm by 1,010 mm prepreg was cut from a roll. Then, the piece was wrapped on to the concrete surface for two layers. Again, the overlap length in the hoop direction was 50 mm. On the top of the prepreg layer, a shrink tape was wrapped in a spiral pattern to apply pressure during curing. Finally, the assembled sample was put into a programmed oven for curing. After curing at 135 °C for 1.5 hours, the repair was completed. Figure 3 shows three repaired samples mounted with uniaxial compressive test fixtures.

For the second type of samples, the same UV curing resin was employed. Unidirectional E-glass fiber was used to reinforce the UV curing resin. The same wet lay-up procedure was utilized and the curing time was also the same as the first type of columns. Six fiber orientations were investigated, as shown in Table 3.

Table 3 Fiber orientations

Fiber orientation	0°/0°	0°/90°	90°/90°	60°/30°	45°/45°	-45°/45°
Number of samples	3	3	3	3	3	3

## 2.5 Specimens Conditioning

For the first type of samples, boiling seawater and UV radiation were used to condition the specimens in order to investigate the hygrothermal durability and the feasibility of the various repairs in maritime structures. The seawater was prepared per ASTM 1183 standard, which contained 2.5 % of NaCl by weight. A 180 × 100 × 60 cm aluminum tank was used as the conditioning chamber. The four sides and the bottom face of the tank were wrapped with insulation foams to reduce the heat loss. The lid was a plate made of 2.5 cm thick plywood to reduce heat dissipation. Two 3 kW PTHF-302 water heaters were used to keep the entire tank of water boiling. A 300 w Mog Base UV lamp was used as the UV radiation source, which had a

wavelength ranging from 280 to 340 nm. Nine repaired samples were moved into the tank and rested in the boiling water for seven days. The conditioning time of one week was chosen to approximately achieve saturation of the FRP layers so that the test results could be used to predict a much longer time of degradation. The 7-day conditioning time was also used in a previous study [13]. Figures 4 (a) and (b) show a layout of the conditioning chamber and specimens in the chamber, respectively. The details of each sample are shown in Table 4.

Table 4 Details of the First Type of Test Samples

Sample Number	Concrete Group	Repair Method	Conditioning	Sample Number	Concrete Group	Repair Method	Conditioning
C1	A	UDC	No	C13	B	UDC	Yes
C2	A	UDC	No	C14	B	DC	Yes
C3	A	DC	No	C15	B	DC	Yes
C4	A	Prepreg	No	C16	B	Prepreg	Yes
C5	A	Prepreg	No	C17	B	Prepreg	Yes
C6	A	Prepreg	No	C18	B	Prepreg	Yes
C7	A	Epoxy	No	C19	B	Epoxy	Yes
C8	A	Epoxy	No	C20	B	Epoxy	Yes
C9	A	Epoxy	No	C21	B	Epoxy	Yes
C10	A	UV curing	No	C22	B	UV curing	Yes
C11	A	UV curing	No	C23	B	UC curing	Yes
C12	A	UV curing	No	C24	B	UV curing	Yes

Note: UDC – Undamaged control sample, DC – Predamaged control sample.

## 2.6 Uniaxial Compression Test

For the first type of samples, all the 24 samples were uniaxially compressed in an Instron MTS machine to determine the modulus of elasticity and compressive strength of various control samples and repaired samples after conditioning,. The modulus of elasticity tests was conducted per ASTM C469 standard. The compressive strength test was conducted by referencing ASTM C 39 standard. The test fixtures were already shown in Fig. 3.

For the second type of samples, the same experiments were also used to test all the 21 specimens.

## 2.7 Residual Mechanical Properties of the FRPs

For the first type of samples, the residual mechanical properties of the FRPs were determined through a tension test in order to better understand the effectiveness of the various repair materials and the environmental conditioning effect. The test coupons, which were 203.2 mm long by 50.8 mm wide, were cut from the repaired samples after the uniaxial compression tests. A rotor cutter was used to cut the coupons along the axial direction. The cutting line was far away from the broken line of the repair layers in order to minimize the possible damages introduced into the coupons during compression tests. Six coupons were prepared from each FRP, three from unconditioned repair and three from conditioned repair. For the three FRPs, a total of 18 coupons were cut, as shown in Fig. 5. The tension test was conducted per ASTM D3096-76 standard via an Instron MTS machine.

### **3. FINITE ELEMENT ANALYSIS**

In order to investigate the effect of fiber orientation the stress-strain distributions, a finite element analysis was conducted in this study.

#### **3.1 Modeling**

A 3-D model of the concrete columns was built using ANSYS®. The cylinder model was built by first modeling 1/36<sup>th</sup> radial sector (10°) of the cylinder. This first sector was used so that a regular radial symmetric mesh can be generated. Once the radial sector was meshed the entire cylinder was generated by repetition of this first sector. The FRP wrapped column was also modeled in the same fashion except a shell element representing the FRP was incorporated into the initial sector. Figure 6 shows a 3-D mesh of an FRP repaired column.

The concrete column was modeled using a special concrete element - SOLID 65. SOLID 65 is an 8-node solid brick element having three translation degrees of freedom per node. This element has crushing (compressive) and cracking (tensile) capabilities. The cracking and crushing failure modes are respectively based on predefined tensile and compressive strength of the concrete. The presence of a crack at an integration point is represented through modification of the stress-strain relations by introducing a plane of weakness in a direction normal to the crack face. Under conditions where crushing has occurred, material strength is assumed to have degraded to an extent such that the contribution to the stiffness of an element at the integration point in question can be ignored. The wrapping FRP layers were modeled using a layered 8-node shell element (SHELL 99). Each node has three translational and three rotational degrees of freedom. A composite laminate of up to 250 layers can be modeled using this shell element. The interfacial bonding between the concrete and the FRP layers was controlled by the number of nodes merged at the interface of the two materials.

#### **3.2 Boundary Conditions and Loading**

The global coordinate system of the cylinder was defined in such a way that the bottom face of the cylinder lay in the x-y plane and the positive z-axis was aligned with the axis of the cylinder. The bottom face of the cylinder was completely clamped (zero displacement and rotation on all nodes at  $z = 0$ ). A pressure load was applied on all nodes on the top face ( $z = h$ ) of the cylinder in a single load step. The load was applied in several sub-steps in such a way that it gradually increased at a constant rate from zero to a predefined final load. Figure 7 shows a cross sectional view of the boundary conditions and the applied pressure.

#### **3.3 Solution and Post Processing**

A non-linear analysis was performed to obtain failure loads and stress/strain data for the column with and without the FRP reinforcement. An iterative approach was used at every sub-step and when the solution converged the calculated parameters (displacement, stress, etc.) were stored in a result data base file.

To track the strain/stress and the failure load, the displacement of two nodes located on the axis of the cylinder was analyzed. The strain was calculated for every sub-step between these two nodes based on the displacement data from the results file. The strain obtained in such a way was plotted against the stress at every sub-step. At the point of failure of the concrete (either

compressive crushing or tensile cracking), the plot showed a sharp break and a substantial drop in modulus of the structure afterwards.

## **4. RESULTS AND DISCUSSION**

### **4.1 Effectiveness of the three FRPs**

The averaged compressive strength and the modulus of elasticity of the various control samples and repaired samples are shown in Figs. 8 – 11, respectively. From Figs. 8 - 11, the following analyses can be conducted.

#### **4.1.1 Effect of Precracking on the Ultimate Capacity of RC Columns**

From Figs. 8 and 9, it is seen that precracking significantly reduced the compressive strength of the RC columns. For the RC columns prepared from concrete batch A (Fig. 8), only 22% of the original compressive strength was retained. For the RC columns prepared from concrete batch B (Fig. 9), only 25% of the original compressive strength was retained. This is because the disintegration of the concrete by the precracking caused a loss of the lateral confinement of the reinforcing steels, considerably reduced the load carrying capacity of the columns. This clearly justifies that repair or jacket of the precracked RC columns is of paramount importance.

#### **4.1.2 Enhancement of the Load Carrying Capacity of Predamaged RC Columns by Externally Bonded FRP Fabrics**

From Fig. 8, it is seen that the repair significantly increased the compressive strength of the predamaged columns. Actually, only two layers of FRPs recovered all the lost compressive strength. The compressive strength of the UV curing resin repaired samples was 4.86 times the strength of the predamaged samples. The compressive strength of the prepreg repaired samples was 5.36 times the strength of the predamaged samples. The compressive strength of the epoxy repaired samples was 5.30 times the strength of the predamaged samples. From the point of view of engineering accuracy, although the UV curing resin repair was a little bit shy compared to the other two repairs, it can be claimed that the two fast repair FRPs have nearly the same strengthening efficiency as the epoxy FRP. Obviously, taking strengthening efficiency as a criterion, heat activated curing prepreg and UV curing resin can replace the long-time curing epoxy.

From Fig. 10, the modulus of elasticity of the prepreg repaired samples was nearly twice that of both the UV curing resin and epoxy repaired samples. This is likely due to a better resin penetration into the cracks and voids of the concrete, as observed in a broken sample shown in Fig. 12. This resin penetration is due to the pressure applied by the shrink tape during the heat activated curing process, resulting in better interfacial bonding. As a result, the stiffness of the prepreg repaired samples was much higher than that of UV curing resin and epoxy repaired samples. It is noted that, however, the good interfacial bonding did not increase the compressive strength considerably. The compressive strength of prepreg repaired samples was only slightly higher than that of the rest repairs, as shown in Fig. 8. This result is in agreement with previous studies in showing that increased interfacial bonding does not significantly increase the compressive strength of a repaired RC column [12]. Even so, a good interfacial bonding is still desirable, particularly for applications where deflection is a limiting factor.

### 4.1.3 Degradation of the Load Carrying Capacity of FRP Repaired RC Columns due to Environmental Conditioning

Subjected to environmental conditioning, the repairs still considerably increased the compressive strength of the predamaged columns, as shown in Fig. 9. Again, only two layers of FRPs recovered all the lost compressive strength. The compressive strength of the UV curing resin repaired samples was 4.15 times the strength of the predamaged samples. The compressive strength of the prepreg repaired samples was 4.44 times the strength of the predamaged samples. The compressive strength of the epoxy repaired samples was 4.39 times the strength of the predamaged samples. Comparing the reinforcing efficiency in Fig. 9 with that in Fig. 8, it is found that environmental conditioning reduced the reinforcing efficiency of the three FRPs. The reduction of the reinforcing efficiency was 14.6 % for UV curing resin, 17.2 % for heat activated curing prepreg, and 17.2 % for ambient environment curing epoxy. The reason for the reduced reinforcing efficiency is that the FRPs are degraded subjected to environmental conditioning. This can be validated by the residual strength test of the FRP coupons cut from the repaired columns. As shown in Table 5, about 12.5 % of the peak load was lost for the UV curing FRP after conditioning. This number became 15.3 % and 14.9 % for the prepreg and epoxy FRP, respectively.

The modulus of elasticity exhibited the same behavior as with the unconditioned samples. From Fig. 11, prepreg repaired samples had a modulus of elasticity nearly twice as many as the modulus of the UV curing resin and epoxy repaired samples. It is noted that the actual values of the conditioned samples are larger than that of the unconditioned samples. This does not mean the conditioning increased the stiffness of the FRPs. Actually, it decreased the stiffness of the FRPs, as shown in Table 5. The larger stiffness of the repaired samples was a result of the stronger batch of concrete used to cast the conditioned batch.

Table 5 Residual Mechanical Properties of FRPs

Materials	Conditioning	Peak Load (KN)	Modulus of Elasticity (GPa)
Epoxy FRP	No	6.12	19.2
	Yes	5.20	17.0
UV curing resin FRP	No	5.50	18.8
	Yes	4.81	16.7
Prepreg FRP	No	6.20	19.8
	Yes	5.25	17.1

The reasons for the degradation of FRPs may be first attributable to the water absorption at elevated temperature, leading to deterioration of the resin matrix and fiber/matrix interfacial bonding. Penetration of water into the FRP occurs by diffusion through the matrix resin and capillary flow via microcracks and voids. Moisture absorption results in development of residual stress and plasticization of the resin. It also leads to debonding at the fiber/matrix interface. The elevated temperature accelerates the water diffusion process and thus leads to rapid degradation of the FRP. Second, the salt may further weaken the fiber/matrix interfacial bonding and attack the E-glass fibers. Third, the ultraviolet radiation may break the chemical bond of organic molecules. Consequently, the matrix may become brittle and matrix cracking and fiber/matrix interfacial debonding may be increased, reducing the mechanical strength of the FRPs. It is

noted that the adverse effect of the conditioning is slightly small for the UV curing resin. This may be because the UV radiation can further cure the resin during conditioning. The reason is that although pure resin can be cured in 20 minutes, E-glass fabric reinforced resin may need a little bit longer time for curing because the fibers may block the penetration of the UV light. As a result, the UV radiation used during conditioning may contribute to further curing the resin.

#### 4.1.4 Failure Mode Analysis

The failure of all the repaired samples was due to the tensile failure of the FRP layers. The failure initiated from about one-eighth to the middle along the height of the columns. Once the crack was initiated, it propagated along the axial direction towards the ends of the sample, as shown in Fig. 13 (a) – (c) with various repairs. Although the failure of the FRPs was a sudden event, the sound from fiber breakage was clearly heard a while before the failure of the FRPs, an indication of warning. After the failure of the FRPs, the broken surface was very rough, a symbol of good fiber/matrix interfacial bonding. In addition, no debonding was observed between the two FRP layers. This means the FRP was well laminated and the construction techniques used in this study were applicable. Furthermore, it was observed that a thin layer of concrete was attached to the FRP layers after failure. This means the three resins had a good bonding with the concrete. They were chemically compatible with concrete. With FRP confinement, only the concrete within the FRP broken zone was disintegrated. The majority of the column was still in an integrated shape.

#### 4.1.5 Cost/Benefit Analysis

As shown in the above results, the benefits of using these repairs in terms of regaining lost strength are virtually identical across the board. A cost/benefit analysis then would fall almost exclusively on the cost, both of the materials and the labor. A break down of the cost of per repaired sample is shown in Table 6.

Table 6 Raw Materials Cost for Repairing Per Column

Repair Method	Item	Cost per Unit	Units Used per sample	Cost per Item	Total Cost per Sample
Epoxy	Epoxy	\$148/L	0.394 L	\$58.31	
	Fabric	\$3.60/m <sup>2</sup>	0.569 m <sup>2</sup>	\$2.05	
					\$60.36
Prepreg	Prepreg Sheet	\$15.79/m <sup>2</sup>	0.569 m <sup>2</sup>	\$8.97	
	Shrink Tape	\$2/roll	0.5 roll	\$1.00	
	Electricity	\$0.08/kWh	9 kWh	\$0.72	
					\$10.69
UV Curing	Resin	\$7.93/L	0.37 L	\$3.00	
	Fabric	\$3.60/m <sup>2</sup>	0.569 m <sup>2</sup>	\$2.05	
					\$5.05

Table 6 considers only the material costs, not including the labor costs and the road user cost due to traffic delay. From Table 6, the two fast curing resins not only have nearly the same strengthening efficiency as the long-time curing epoxy, but are also very cost-effective. If the labor cost and the road user cost were taken into account, the heat activated curing prepreg and the UV curing resin would become even more economically desirable. For field level repair, it is very difficult to provide the heat to cure the prepreg. Therefore, even though prepreg repaired samples showed the maximum strength and stiffness, UV curing resin is a more preferable choice.

#### **4.2 Fiber orientation effect – finite element analysis**

Figure 14 shows the effect of fiber orientation on the stress-strain curves. It can be observed that the stress-strain curve is characterized by three sections. The first section corresponds to the stress-strain curve before the concrete fails. In this section, the effect of the fiber wraps is minimal. The FRP wrapped concrete columns behave similar to those without FRP wraps. Immediately following the first part, a transition zone appears. In this section, the concrete is damaged gradually and continuously with the increase of the applied load. As the load increases, the concrete undergoes tensile cracking, mixed tensile cracking and compressive crushing until total crushing of the concrete. Figure 15 (a) – (c) show such a progressive damage and the associated stresses. In Fig.15, the circle represents cracking and the polygon represents crushing. It is noted that this section was not shown in previous studies by others. The reason may be that they used a wider range of strain (up to 0.02) so that this section (with strain range from 0.001 – 0.005) was undetected. Therefore, they failed to show the delicate details of this transition zone and claimed that it was a sharp turning point [20]. In this part, two opposite mechanisms are taking effect. On one hand, the concrete degrades gradually, resulting in continuous drop in stiffness; on the other hand, the FRP wraps are activated progressively due to the dilation and expansion of the confined concrete. Once the concrete is totally crushed, the FRP wraps are fully activated. This leads to the third section.

From Fig. 14, it is seen that, with perfect FRP/concrete interfacial bonding, the fiber orientation has a considerable effect on the stress-strain curve (solid lines in Fig. 14). As contrary to general assumptions that fibers should be aligned along the hoop direction, this analysis shows that it will be more effective if fibers are aligned along axial direction. This is understandable because, with perfect interfacial bonding, the FRP wraps are in biaxial stress conditions. The axial load applied to the core concrete will be transferred to the FRP wraps through the interfacial bonding. In addition, some of the load will be directly applied to the FRP wraps along the axial direction. Therefore, it is very likely that the axial direction is an orientation which needs particular care. The fibers should be aligned along the axial direction. With the weakness of the interfacial bonding, the axial load transferred to the FRP wraps becomes less and less. The difference between the axial direction fibers and hoop direction fibers will become less and less. If there is no interfacial bonding and no interfacial frictional force, the difference will almost disappear. This is exactly the case from the analysis. It is seen in Fig. 14 that, without interfacial bonding and interfacial frictional force, the stress-strain curves for different fiber orientations are almost overlapped (dashed line in Fig. 14). The effect of the fiber orientation can be neglected. It is noted that the interfacial bonding and the interfacial frictional forces cannot be zero in practice, thus the fiber orientation will always play a certain role. As shown in this study, fibers in axial direction will be more effective than fibers in hoop

direction. It is worth mentioning that this conclusion is based on the particular FRP repaired concrete columns in this study. Refined studies are needed in order to fully validate this conclusion.

### 4.3 Fiber orientation effect – experimental investigation

The averaged test results of compressive strength, compressive modulus of elasticity, and Poisson’s ratio are summarized in Table 7.

Table 7 Summary of test results

Fiber orientation	Compressive strength (MPa)	Modulus of elasticity (GPa)	Poisson’s ratio
0°/0°	49.40	35.09	0.22
0°/90°	48.67	36.99	0.22
90°/90°	47.61	37.48	0.21
60°/30°	46.12	35.41	0.24
45°/45°	46.72	37.29	0.24
-45°/45°	46.75	36.34	0.23
Control	45.95	35.20	0.24

Compared to the control samples, i.e., samples without FRP wraps, the wrapped samples show a slightly higher compressive strength and stiffness. This is within the expectations of this study. It is interesting to note that the effect of fiber orientation on the strength and stiffness is different. For the compressive strength, fibers aligned in hoop direction (0°/0°) yield the highest strength. This is in agreement with FRP repaired columns, where hoop direction is the optimal direction. Because hoop direction is the optimal direction, it is inferred that the compressive strength will decrease as the fibers align more and more towards the axial direction, and the lowest compressive strength will occur when fibers are aligned along axial direction (90°/90°). The test results do not support this inference. The compressive strength is not the lowest when fibers are aligned along the axial direction. A possible reason is that the applied load is not perfectly along the axial direction. Eccentricity cannot be avoided. This eccentricity introduces a bending moment to the wrapped column. It is well known that fibers in the axial direction are optimal to resist this bending moment. Therefore, fibers in axial direction do not yield the lowest compressive strength.

For the compressive modulus of elasticity, fibers in axial direction yield the highest stiffness, while fibers in hoop direction display the lowest stiffness. Therefore, the most optimal fiber direction for strength is the least optimal direction for stiffness.

Considering that it cannot be avoided that concrete columns in bridges will be subjected to a certain bending moment, it is desirable that some fibers be aligned along axial direction. Fibers aligned along hoop direction only are not the best design. Based on the relative magnitude of the axial compressive load and the bending moment, fibers along 0°/90° or along 90° only may become the optimal fiber direction. More refined studies are needed to find the optimal fiber direction.

## 5. CONCLUSIONS

In this study, precracked RC columns were repaired by three types of FRPs ranging from very fast curing to long time curing. The detailed repair processes were presented in the study. Accelerated conditioning was also used to evaluate the hygrothermal durability of the various repairs. Uniaxial compressive test was conducted on the conditioned specimens and control samples to determine the compressive strength and modulus of elasticity. A tension test was also conducted on the FRP coupons cut from the repaired samples to determine their residual mechanical properties. Through the testing of a total of 24 RC columns and 18 FRP coupons, the following preliminary conclusions are obtained:

- The two fast curing resins achieved nearly the same reinforcing efficiency as the long-time curing resin with a much lower cost. It is recommended that the two fast curing resins can replace the long-time curing epoxy in repairing damaged RC columns. The UV curing resin is even more desirable considering its low cost and the ease of construction.
- While good interfacial bonding does not increase the overall compressive strength of the repaired samples to a noticeable degree, it does increase the stiffness significantly.
- Deterioration due to hygrothermal conditioning was least in the UV curing resins (roughly 14.2%), but was fairly consistent between the samples (about 17.2% for the heat-curing prepreg and the ambient environment curing epoxy).
- The FRPs were well prepared by the construction techniques used in this study. The three resins were chemically compatible with the concrete.

In this study, a finite element analysis using ANSYS<sup>®</sup> was also implemented and twenty-one plain concrete columns were also prepared to investigate the effect of fiber orientation on the stress-strain distributions. Based on the finite element modeling and test results, the following preliminary conclusions are obtained:

- The stress-strain curve is characterized by three distinct regions. There is a transition zone between the first region where the FRP wraps are dormant and the third region where the FRP layers are fully activated.
- The effect of the fiber orientation on the strength and stiffness is coupled with the effect of the interfacial bonding. With perfect interfacial bonding, fibers in axial direction are more effective than those in hoop direction; with weak interfacial bonding, however, the effect of fiber orientation can be neglected.
- For field columns, fibers along  $0^{\circ}/90^{\circ}$  or along  $90^{\circ}$  only may become the optimal fiber direction. Fibers along the hoop direction ( $0^{\circ}$ ) only may not be the optimal fiber orientation.

## ACKNOWLEDGMENTS

This investigation was partially sponsored by the Mack-Blackwell Transportation Center at the University of Arkansas under project number 2033. Louisiana Transportation Research Center (LTRC) Concrete and Structures Lab helped cast the concrete columns and conduct the tests. Mr. Randy Young, Mr. Matt Tircuit, and Mr. Alvin Mix III from LTRC, Mr. Samuel Kidane, Mr. Jerry Peck, and Mr. Nikhil Gupta from LSU Mechanical Engineering, Mr. Scott Hedlund from LSU Civil and Environmental Engineering, and Mr. Kevin Ordoyne from LSU Marine Services Shop assisted in the tests. Their assistance is greatly appreciated.

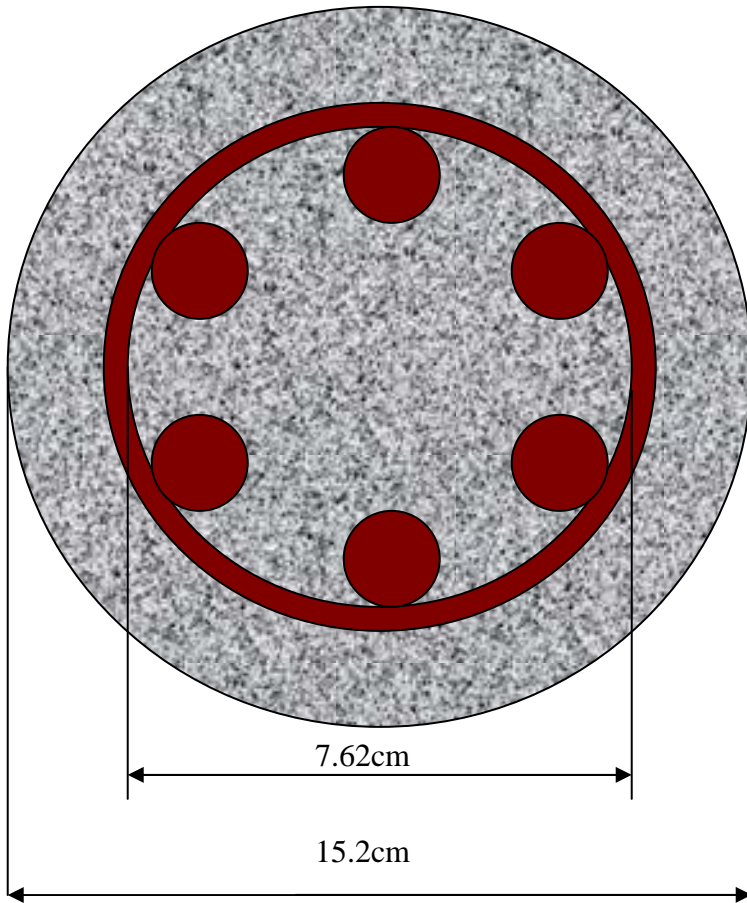
## REFERENCES

- [1] F.W. Klaiber, K.F. Dunker, T.J. Wipf, and W.W. Sanders, Jr., "Methods of Strengthening Existing Highway Bridges," *National Cooperative Highway Research Program Report, 293, Transportation Research Board*, Washington, D.C., (1987).
- [2] S.J. Pantazopoulou, J.F. Bonacci, S. Sheikh, M.D.A. Thomas, and N. Hearn, "Repair of Corrosion-Damaged Columns with FRP Wraps," *Journal of Composite for Constructions*, Vol. 5, No. 1, 2001, pp3-11.
- [3] A.S. Debaiky, M.F. Green, and B.B. Hope, "Carbon Fiber-Reinforced Polymer Wraps for Corrosion Control and Rehabilitation of Reinforced Concrete Columns," *ACI Materials Journal*, Vol. 99, No. 2, 2002, pp. 129-137.
- [4] I. Nishizaki and S. Meiarashi, "Long-term Deterioration of GFRP in Water and Moist Environment," *Journal of Composite for Constructions*, Vol. 6, No. 1, 2002, pp. 21-27.
- [5] S. Pessiki, K.A. Harries, J.T. Kestner, R. Sause, J.M. Ricles, "Axial Behavior of Reinforced Concrete Columns Confined with FRP Jackets," *Journal of Composite for Constructions*, Vol. 5, No. 4, 2001, pp. 237-245.
- [6] A. Parvin and W. Wang, "Behavior of FRP Jacketed Concrete Columns under Eccentric Loading," *Journal of Composite for Constructions*, Vol. 5, No.3, 2001, pp.146-152.
- [7] Y.C. Kog, K.C.G. Ong, C.H. Yu, and A.P.V. Sreekanth, "Reinforced Concrete Jacketing for Masonry Columns with Axial Loads," *ACI Materials Journal*, Vol. 98, No. 2, 2001, pp. 105-115.
- [8] H. Toutanji and Y. Deng, "Performance of Concrete Columns Strengthened with Fiber Reinforced Polymer Composite Sheet," *Advanced Composite Materials*, Vol. 10, No. 2-3, 2001, pp. 159-168.
- [9] S. Zhang, L. Ye, Y. -W. Mai, "Effects of Saline Water Immersion on Glass Fiber/Vinyl-Ester Wrapped Concrete Columns," *Journal of Reinforced Plastics and Composites*, Vol. 18, No. 17, 1999, pp. 1592-1604.
- [10] H.A. Toutanji, "Stress-Strain Characteristics of Concrete Columns Externally Confined with Advanced Fiber Composite Sheets," *ACI Materials Journal*, Vol. 96, No. 3, 1999, pp. 397-404.
- [11] H. Saadatmanesh, M.R. Ehsani, and L. Jin, "Repair of Earthquake-Damaged RC Columns with FRP Wraps," *ACI Structural Journal*, Vol. 94, No. 2, 1997, pp. 206-215.
- [12] M. Shahawy, A. Mirmiran, and T. Beitelman, "Tests and Modeling of Carbon-Wrapped Concrete Columns," *Composites Part B: Engineering*, Vol. 31B, No. 6/7, 2000, pp. 471,480.
- [13] G. Li, D. Mukai, S. -S. Pang, J.E. Helms, S.I. Ibekwe, and W. Alaywan, "Structural Degradation of FRP Strengthened RC Beams Subjected to Hygrothermal and Aging Attacks," *Journal of Composite Materials*, Vol. 36, No. 7, 2002, pp. 795-812.
- [14] S.H. Ahn and G.S. Springer, "Repair of Composite Laminates-I: Test Results," *Journal of Composite Materials*, Vol. 32, No. 11, 1998, pp. 1036-1074.
- [15] S.H. Myhre and J.D. Labor, "Repair of Advanced Composite Structures," *Journal of Aircraft*, Vol. 18, 1980, pp. 546-552.
- [16] C. Bachmann, "UV Structural Adhesives and Sealants - How They Are Unique in the Larger Universe of Photocuring Resins," *Adhesive Age*, Vol. 42, No. 4, 1999, pp. 24-31.
- [17] M.S. Sennett and S.E. Wentworth, "Evaluation of Resins Cured by Ultraviolet Radiation and in Conjunction with Fiber Optic Systems for use in the Field Repair of Composite Materials," MTL-TR-87-15, March 1987, ADA181256.

- [18] G. Li, N. Pourmohamadian, A. Cygan, J. Peck, J. E. Helms, and S.S. Pang, “Fast Repair of Laminated Beams Using UV Curing Composites,” *Composite Structures*, Vol. 60, No. 1, pp. 73-81, 2003.
- [19] T. Uomoto, H. Mutsuyoshi, F. Katsuki, and S. Misra, “Use of Fiber Reinforced Polymer Composites as Reinforcing Materials for Concrete,” *Journal of Materials in Civil Engineering*, Vol. 14, No. 3, 2002, pp. 191-209.
- [20] C.E. Bakis, L.C. Bank, V.L. Brown, E. Cosenza, J.F. Davalos, J.J. Lesko, A. Machida, S.H. Rizkalla, and T.C. Triantafillou, “Fiber Reinforced Polymer Composites for Construction – State-of-the-Art Review,” *Journal of Composites for Construction*, Vol. 6, No. 2, 2002, pp. 73-87.
- [21] M. Samaan, A. Mirmiran, and M. Shahawy, “Model of Concrete Confined by Fiber Composites,” *Journal of Structural Engineering*, ASCE, Vol. 124, No. 9, 1998, pp. 1025-1031.
- [22] G. Li, S.S. Pang, E. Woldesenbet, M. Stubblefield, P.F. Mensah, and S.I. Ibekwe, “Investigation of Preperg Bonded Composite Single-Lap Joint,” *Composite Part B: Engineering*, Vol. 32, No. 8, 2001, pp. 651-658.

## FIGURES

- Figure 1** (a) Schematic cross sectional design of steel reinforcement and (b) Actual steel reinforcement
- Figure 2** (a) Split tensile test and (b) cracks resulting from split tensile test
- Figure 3** (a) Epoxy repaired sample in compression test, (b) prepreg repaired sample in compression test, and (c) UV curing resin repaired sample in compression test
- Figure 4** (a) Conditioning tank with heaters and UV lamp and (b) samples in conditioning tank
- Figure 5** FRP coupons from repaired samples for residual tensile test
- Figure 6** Three-dimension mesh
- Figure 7** A schematic of boundary conditions and applied pressure
- Figure 8** Averaged compressive strength of various samples without conditioning
- Figure 9** Averaged compressive strength of various samples with conditioning
- Figure 10** Averaged modulus of elasticity of repaired samples without conditioning
- Figure 11** Averaged modulus of elasticity of repaired samples with conditioning
- Figure 12** Penetration of resin into cracks from prepreg repaired sample
- Figure 13** (a) Failure of epoxy repaired sample, (b) Failure of UV curing resin repaired sample, and (c) Failure of prepreg repaired sample
- Figure 14** Effect of fiber orientation on the stress-strain behavior
- Figure 15** Progressive damages in concrete



(a) Schematic of cross sectional design of steel reinforcement

(b) Actual steel reinforcement

Figure1 (a) Schematic cross sectional design of steel reinforcement and (b) Actual steel reinforcement



(a) Split tensile test



(b) Induced cracks

Figure 2 (a) Split tensile test and (b) cracks resulting from split tensile test



(a) Epoxy repaired sample



(b) Prepreg repaired sample



(c) UV curing resin repaired sample

Figure 3 (a) Epoxy repaired sample in compression test, (b) prepreg repaired sample in compression test, and (c) UV curing resin repaired sample in compression test



(a) Conditioning tank



(b) Samples in the tank

Figure 4 (a) Conditioning tank with heaters and UV lamp and (b) samples in conditioning tank

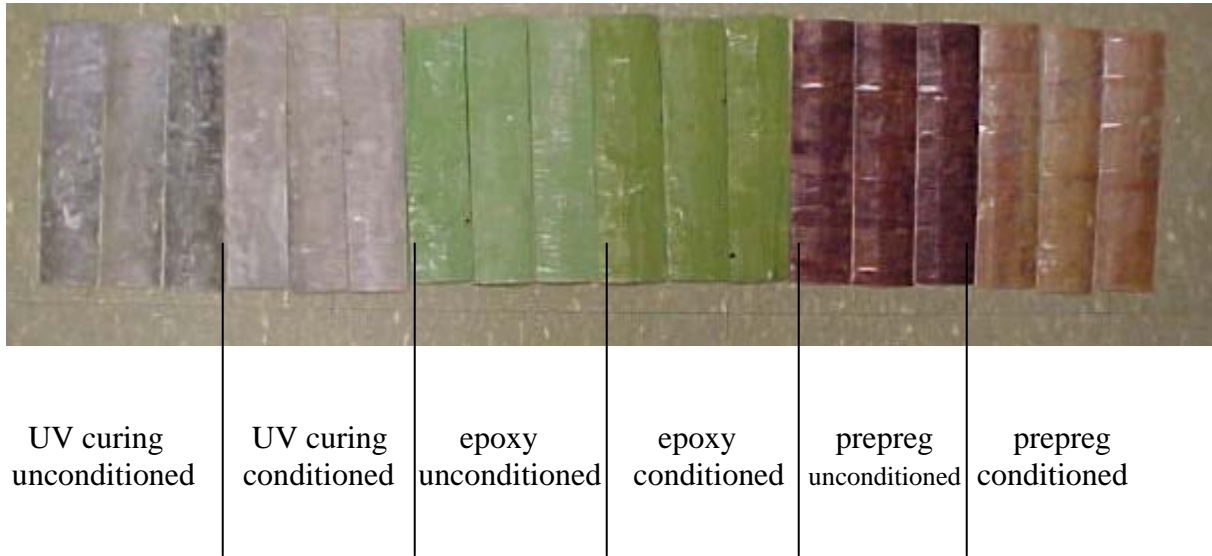


Figure 5 FRP coupons from repaired samples for residual tensile test

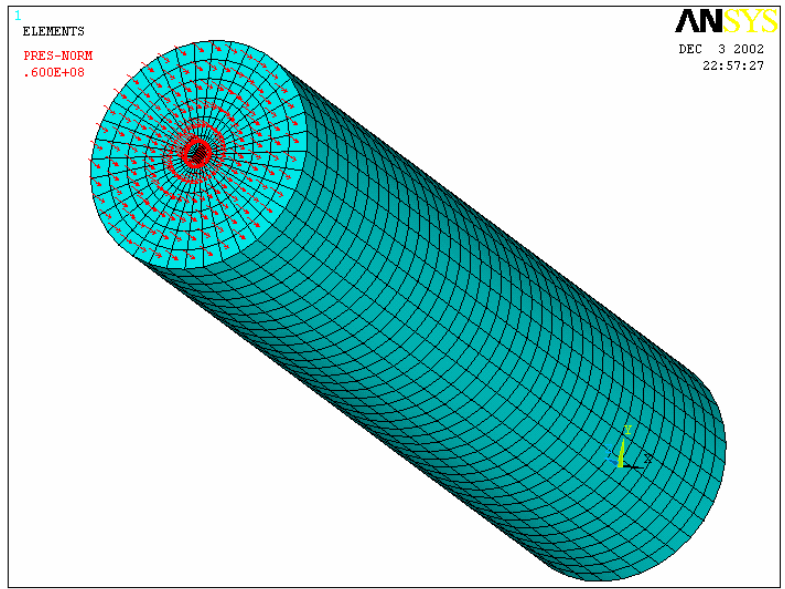


Fig. 6 Three-dimension mesh

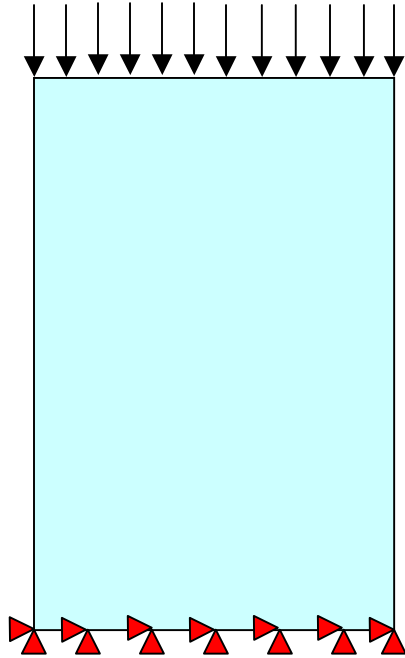


Fig. 7 A schematic of boundary conditions and applied pressure

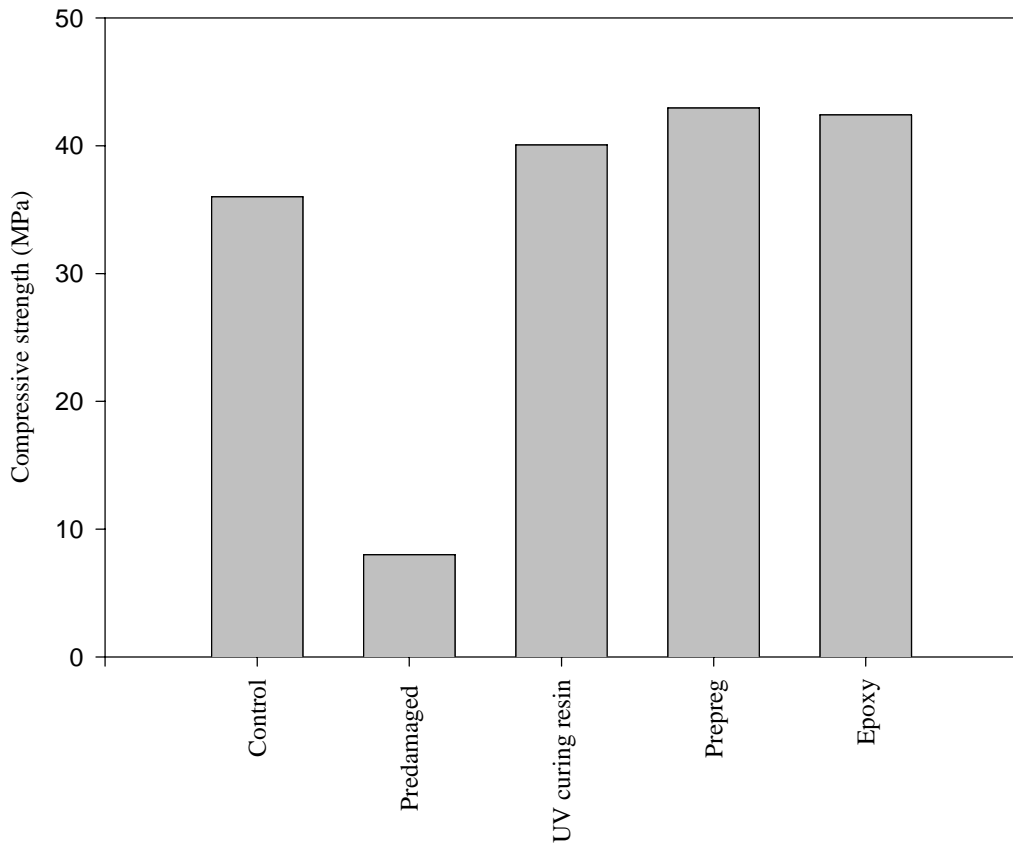


Fig. 8 Averaged compressive strength of various samples without conditioning

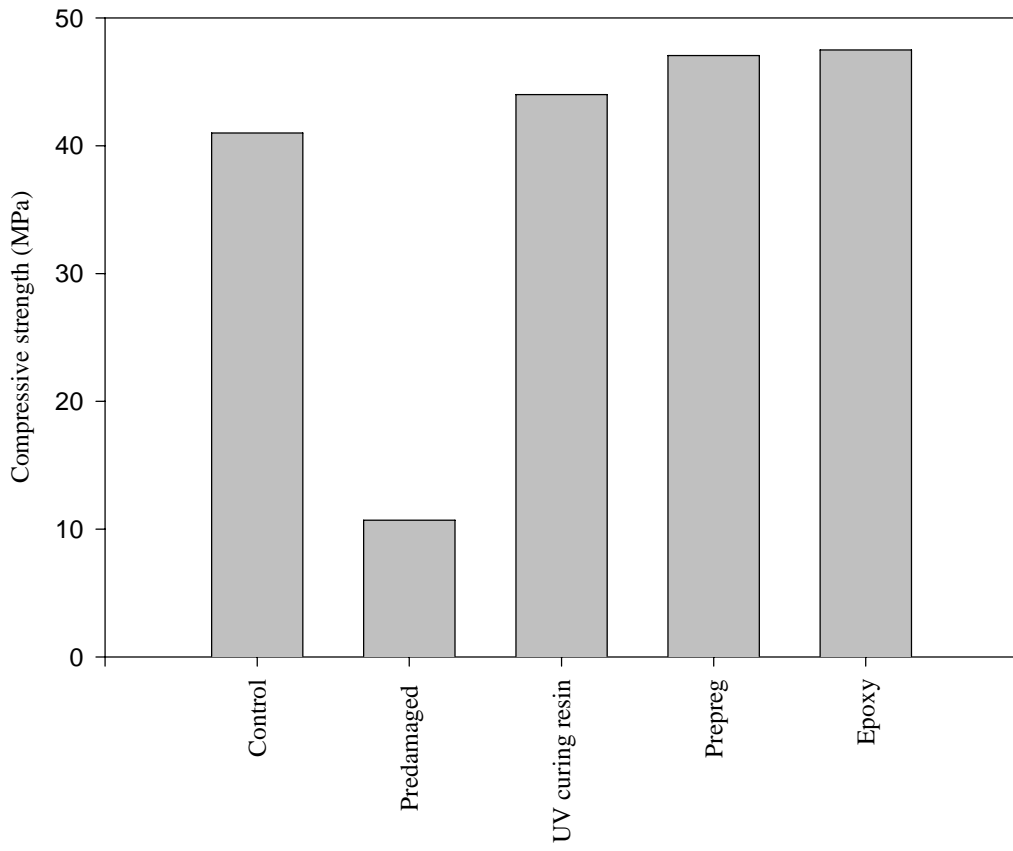


Fig. 9 Averaged compressive strength of various samples with conditioning

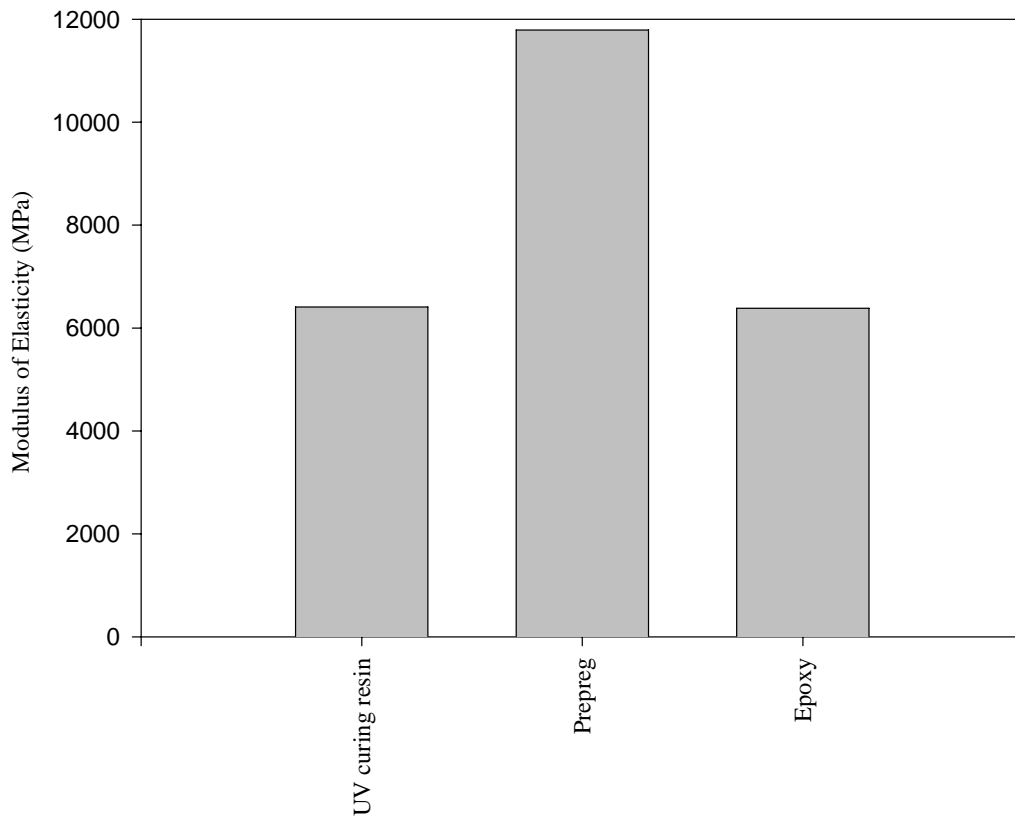


Fig. 10 Averaged modulus of elasticity of repaired samples without conditioning

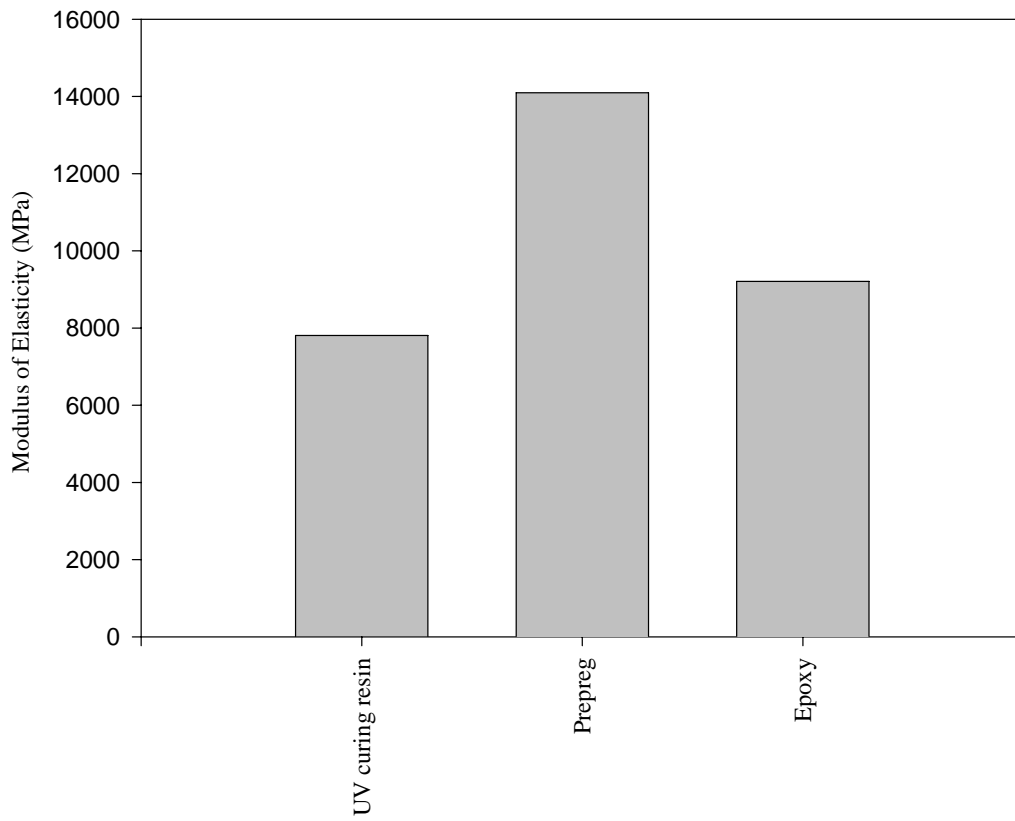


Fig. 11 Averaged modulus of elasticity of repaired samples with conditioning



Figure 12 Penetration of resin into cracks from prepreg repaired sample



(a)



(b)



(c)

Figure 13 (a) Failure of epoxy repaired sample, (b) Failure of UV curing resin repaired sample, and (c) Failure of prepreg repaired sample

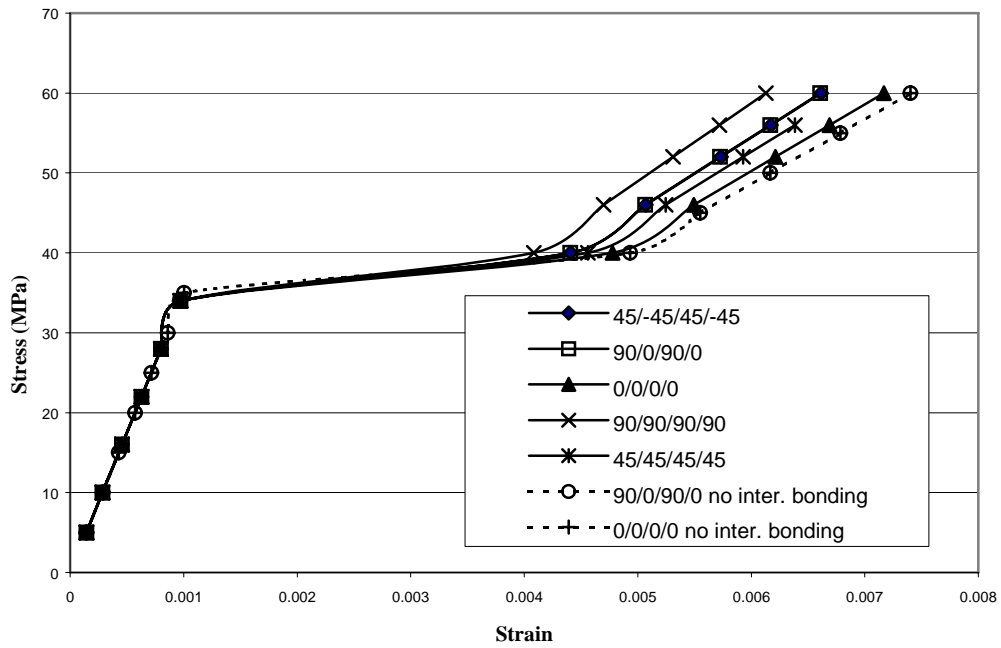
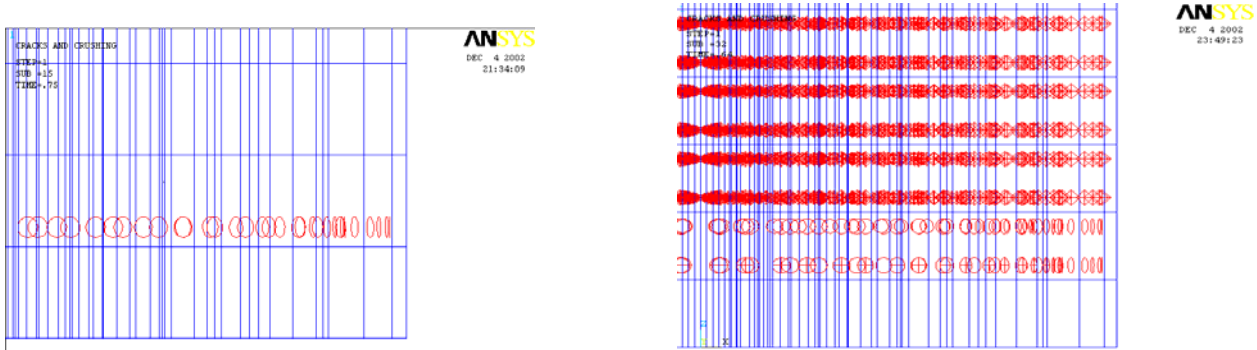
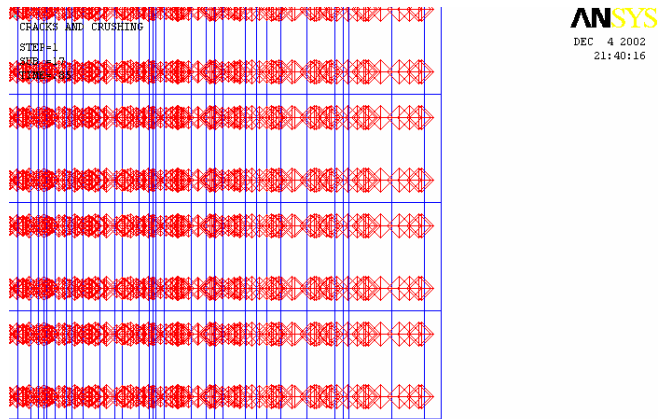


Fig. 14 Effect of fiber orientation on the stress-strain behavior



(a) Tensile crack at 35.2 MPa applied pressure (b) Mixed tensile crack and compressive crush at 38.7 MPa pressure



(c) Fully concrete crush at 42.0 MPa applied pressure

Fig. 15 Progressive damages in concrete